Chemical Science

EDGE ARTICLE

View Article Online
View Journal | View Issue

CrossMark click for updates

Cite this: *Chem. Sci.*, 2015, **6**, 3544

Addressing, amplifying and switching DNAzyme functions by electrochemically-triggered release of metal ions

Lina Freage,†[a] Alexander Trifonov,†[a] Ran Tel-Vered,[a] Eyal Golub,[a] Fuan Wang,[a] John S. McCaskill[b] and Itamar Willner*[a]

Received 1st March 2015
Accepted 8th April 2015

DOI: 10.1039/c5sc00744e

www.rsc.org/chemicalscience

The design of artificial cells, which mimic the functions of native cells, is an ongoing scientific goal. The development of stimuli-responsive chemical systems that stimulate cascaded catalytic transformations, trigger chemical networks, and control vectorial branched transformations and dose-controlled processes, are the minimum requirements for mimicking cell functions. We have studied the electrochemical programmed release of ions from electrodes, which trigger selective DNAzyme-driven chemical reactions, cascaded reactions that self-assemble catalytic DNAzyme polymers, and the ON–OFF switching and dose-controlled operation of catalytic reactions. The addressable and potential-controlled release of Pb^{2+} or Ag^{+} ions into an electrolyte that includes a mixture of nucleic acids, results in the metal ion-guided selection of nucleic acids yielding the formation of specific DNAzymes, which stimulate orthogonal reactions or activate DNAzyme cascades.

The design of artificial cells is a major scientific challenge that has attracted substantial research efforts in the last two decades.[1,2] Different approaches to construct simple, cell-like structures for specific applications have been reported.[3–6] Different components have been integrated with cell-mimetic compartments, and the implementation of these constructs to drive complex transformations has been discussed.[7,8] Although important scientific progress in developing building units of artificial cells has been reported, an operational man-made cell is still an unresolved goal. Different challenges exist in developing artificial cells. These include the fabrication of membrane-like compartments,[9,10] the development of amplification feedback mechanisms and cascaded chemical transformations responding to environmental stimuli,[11] and the replication of the cell configuration and its constituent parts.[12,13] Tackling these issues would allow for the construction of complex chemical networks capable of controlling vectorial branched transformations, dose-controlled processes, oscillatory reactions *etc.* By studying the electrochemical properties of electrodes, and the triggering of specific chemical transformations by electrical stimuli to the extent that cell-like systems are duplicated, might provide a basis to construct "electronic cells".[14] That is, the addressable, potential-induced release of different ions, the local electrically-stimulated pH changes that control the local electrical properties at the electrodes, or the separation of molecular/biomolecular complexes, which regulate chemical transformations and catalytic cascades might provide important steps towards an electronic cell. Although substantial research efforts to develop "artificial cells" have been reported, limited advances have been made and the concept remains a scientific "holy grail". Here we report the first step to develop an electronic (electrochemical) cell that highlights the electrical addressing of the electrodes, the release and uptake of metal ions from the electrodes, the subsequent control of catalytic nucleic acids (DNAzymes), and the activation of DNAzyme cascades. Specifically, the electrically-triggered, dose-controlled release of the ions allows for the regulation of secondary DNAzyme-catalyzed reactions.

Catalytic nucleic acids, DNAzymes, have attracted recent research efforts as catalytic labels for amplifying sensing events,[15–19] as catalysts for the activation of DNA machines,[20–22] and as building blocks for the assembly of nanostructures.[23] Specifically, metal ion-dependent DNAzymes that stimulate the hydrolytic nicking of nucleic acids,[24–26] and hemin/G-quadruplex horseradish peroxidase-mimicking DNAzymes were reported.[27–29] In the present study, we electrically trigger the release of Pb^{2+} and Ag^{+} ions from electrode surfaces, thereby activating the secondary Pb^{2+}-dependent DNAzyme[30–32] and the hemin/G-quadruplex DNAzyme, respectively. We demonstrate the cyclic and reversible electrical "ON"/"OFF" activation and deactivation of the DNAzymes, and highlight the DNAzyme-driven operation of a catalytic cascade that synthesizes polymeric DNAzyme wires.

[a]*Institute of Chemistry, The Hebrew University of Jerusalem, Jerusalem, 91904, Israel. E-mail: willnea@vms.huji.ac.il*

[b]*Biomolecular Information Processing (BioMIP), Ruhr-Universität Bochum, Universitätsstr 150, Bochum, 44801, Germany*

† Equally contributed to this study.

Results and discussion

The study is based on the electrochemical deposition of layers of Pb^0 and/or Ag^0 on Au supports. These layers act as metallic reservoirs that can be stripped off from the electrodes upon the application of specific bias potentials. Fig. 1, curves (a) and (b), depicts the linear sweep voltammograms (LSVs) corresponding to the stripping of the Pb^{2+} or the Ag^+ ions from the Pb^0 or Ag^0 reservoirs, respectively. Fig. 1, curve (c), shows an LSV corresponding to the stripping of both Pb^{2+} and Ag^+ from an electrode which contains the two metal reservoirs. The results imply that upon application of a potential higher than −0.6 V *vs.* the Ag quasi-reference electrode (QRE), Pb^{2+} ions are released from the Pb^0-deposited surface, whereas application of a potential higher than 0.1 V *vs.* the Ag QRE oxidizes the Ag^0 reservoir and releases Ag^+ ions. Subjecting the electrode that includes the two metallic reservoirs to a potential higher than 0.1 V *vs.* the Ag QRE, results in the release of both metal ions from the electrode. Furthermore, the potential applied on the electrode determines the specific metal which is oxidized to the solution and the extent of the release process, while the amount of released metal ions can also be controlled by the time-interval of the applied potential step. Therefore, this potential-induced release of metal ions from the electrode can then be designed to electrochemically trigger interactions between these metal ions and nucleic acids solubilized in the electrolyte. Specifically, our study demonstrated that electrochemically-released Pb^{2+} ions triggered the operation of the Pb^{2+}-dependent DNAzyme and that the electrochemical release of Ag^+ ions cooperatively stabilized a DNA duplex through the formation of cytosine–Ag^+–cytosine (C–Ag^+–C) bridges.

Fig. 2(A) depicts the electrically-controlled activation of the Pb^{2+}-dependent DNAzyme. Lead was deposited on a Au electrode and served as the source of Pb^{2+}. The Pb^0-functionalized electrode was immersed in an electrolyte solution that included the Pb^{2+}-dependent DNAzyme sequence (**1**) and its fluorophore/quencher (ROX/BH2)-functionalized substrate, (**2**). Subjecting the electrode to a potential step from −0.6 V to −0.2 V *vs.* the Ag quasi-reference electrode (QRE) resulted in the stripping of the Pb^{2+} ions into the solution. The time interval of the applied potential pulse controlled the amount of released Pb^{2+}, which activated the Pb^{2+}-dependent DNAzyme, catalyzing the nicking of the substrate (**2**). The cleavage of (**2**) was transduced by the fluorescence of the fluorophore, arising from the separation of the fluorophore from the quencher. Fig. 2(B), curves (a) to (c), depicts the time-dependent fluorescence changes of the system subjected to potential steps of different time intervals. As the time interval of the potential step is increased, the time-dependent fluorescence changes, as a result of the cleavage of (**2**), are intensified, consistent with a higher amount of released Pb^{2+} ions. The fact that no fluorescence changes are observed, implies that the potential-induced release of Pb^{2+} ions is essential for the activation of the

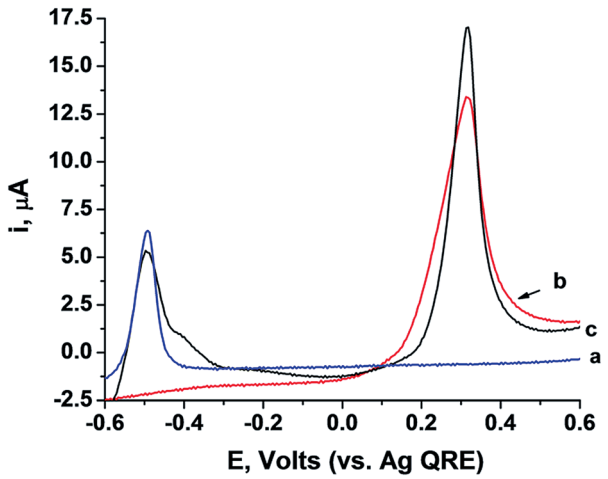

Fig. 1 Linear sweep voltammograms (LSVs) corresponding to the electrochemical release of: (a) Pb^{2+} ions from a Pb^0 reservoir associated with an electrode, (b) Ag^+ ions from a Ag^0 reservoir associated with an electrode, and (c) both Pb^{2+} and Ag^+ ions from a Pb^0/Ag^0 reservoir deposited on an electrode. All measurements were performed in a HEPES buffer (0.05 M, pH = 7.0) containing NaCl, 50 mM. Scan rate: 100 mV s^{-1}.

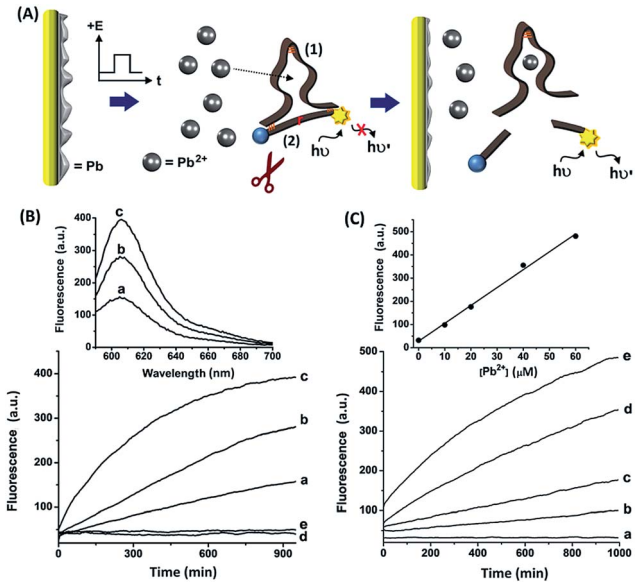

Fig. 2 (A) Electrochemically-triggered activation of the Pb^{2+}-dependent DNAzyme. (B) Time-dependent fluorescence changes, at $\lambda = 590$ nm, as a result of the Pb^{2+}-stimulated, DNAzyme cleavage of (**2**) upon subjecting the electrode to potential pulses at −0.2 V *vs.* the Ag QRE for different time-intervals: (a) 1, (b) 2, and (c) 3 s. Curve (d) corresponds to the time-dependent fluorescence changes of the system in the absence of an applied potential, and curve (e) shows the time-dependent fluorescence changes of the system upon applying a potential of −0.2 V *vs.* the Ag QRE for 3 s with Na_2S, 65 mM, added to the system. Top: fluorescence spectra of the systems described in curves (a)–(c) generated after 950 minutes. (C) Time-dependent fluorescence changes upon the manual activation of the Pb^{2+}-dependent DNAzyme in the presence of variable Pb^{2+} concentrations: (a) 0, (b) 10, (c) 20, (d) 40, and (e) 60 μM Pb^{2+}. Top: derived calibration curve corresponding to the fluorescence of the system generated at different concentrations of added Pb^{2+} ions after a fixed time interval of 1000 min. All measurements were performed in a HEPES buffer solution (0.05 M, pH = 7.0) containing NaCl, 50 mM, (**1**), 1 μM, and (**2**), 0.75 μM.

DNAzyme. Fig. 2(B), curve (d), shows the time-dependent fluorescence changes of the system without applying the potential to release the Pb^{2+} ions. Introduction of Na_2S into the electrolyte solution results in the precipitation of the electrically-released Pb^{2+} ions in the form of PbS, leading to the blocking of the DNAzyme activity, as shown in Fig. 2(B), curve (e). Evidently, no fluorescence changes are observed in the absence of the metal ions. Fig. 2(B), top, shows the emission spectra recorded after the application of the oxidation potential pulse for different time intervals. These results confirm that the electrically-released Pb^{2+} ions activate the catalytic functions of the DNAzyme.

We further examined the catalytic activity of the Pb^{2+}-dependent DNAzyme towards the hydrolytic cleavage of (**2**) by manually adding Pb^{2+} ions to vary the Pb^{2+} concentration. Fig. 2(C) depicts the time-dependent fluorescence changes upon subjecting the mixture of (**1**) and (**2**) to solutions containing variable concentrations of Pb^{2+} ions. As the concentration of Pb^{2+} ions increases, the fluorescence changes are intensified, consistent with the higher activity of the Pb^{2+}-dependent DNAzyme at elevated concentrations of Pb^{2+} ions. Fig. 2(C), top, depicts the calibration curve corresponding to the fluorescence intensities generated by the system after a fixed time interval of 1000 minutes, as a function of the concentration of the manually added Pb^{2+} ions. The derived calibration curve allows us to evaluate the concentrations of Pb^{2+} released upon applying the oxidation pulses of 1, 2, and 3 seconds to be 16, 33, and 50 μM, respectively. Coulometric analyses of the electrical release of Pb^{2+} during the three time interval pulses revealed the associated charges to be 1.0, 1.8, and 2.5 mC. Hence, the current efficiencies for the release of the Pb^{2+} ions corresponded to 62, 70, and 77%, respectively.

We next attempted to activate a different DNAzyme through the electrically-driven release of another ion, Ag^+. This is exemplified in Fig. 3(A), which shows the electrically-triggered release of Ag^+ ions and the activation of the hemin/G-quadruplex horseradish peroxidase-mimicking DNAzyme. The design of this system is based on the following elements: (i) Ag^+ ions form cytosine–Ag^+–cytosine complexes, and these cooperatively stabilize the formation of duplex nucleic acid structures,[33] (ii) subunits of the G-quadruplex sequence can self-assemble in the presence of K^+ to yield G-quadruplexes.[34,35] The quadruplexes can be stabilized by cooperative duplex domains between the subunits. Accordingly, we designed two nucleic acids, (**3**) and (**4**), that included the G-quadruplex domains I and II, and the domains III and IV that include partial complementary sequences and two C–C mismatches, respectively. Under the experimental conditions, the strands (**3**) and (**4**) do not assemble into a stable G-quadruplex, and the formation of the hemin/G-quadruplex DNAzyme is prohibited. The electrically-triggered release of Ag^+ ions from the electrode results in the formation of stable C–Ag^+–C-bridged duplexes between domains III/IV of (**3**)/(**4**), resulting in the synergistic stabilization of the G-quadruplex. The incorporation of hemin into the G-quadruplex then yields the catalytically-active hemin/G-quadruplex DNAzyme. The activity of the DNAzyme is followed by the DNAzyme-catalyzed oxidation of 2,2′-azino-bis(3-ethylbenzothiazoline-6-sulphonic acid), $ABTS^{2-}$, by H_2O_2, and the

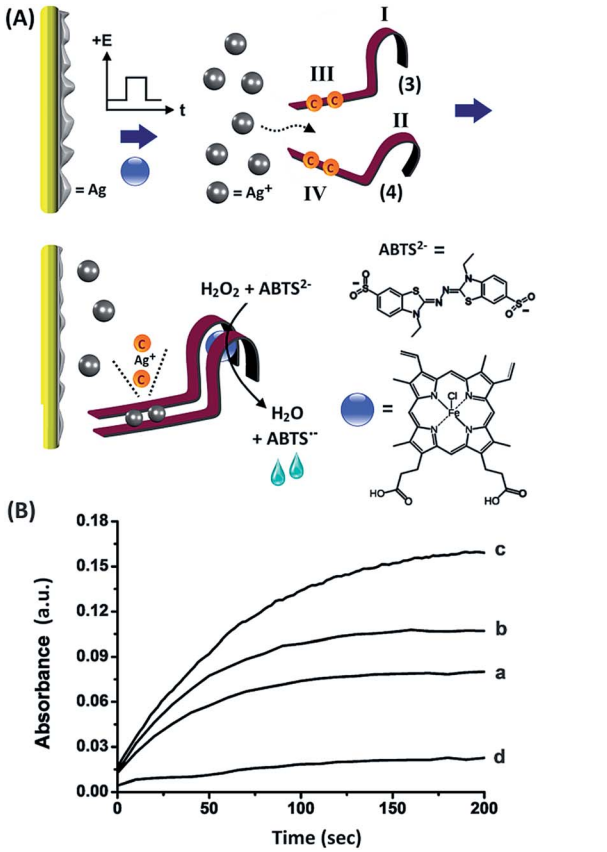

Fig. 3 (A) Electrochemically-triggered release of Ag^+ ions resulting in the activation of an HRP-mimicking DNAzyme by the Ag^+ ion-induced assembly of a hemin/G-quadruplex structure. (B) Time-dependent absorbance changes, at $\lambda = 415$ nm, as a result of the DNAzyme-catalyzed oxidation of $ABTS^{2-}$ by H_2O_2. The oxidation of Ag was carried out by the application of potential pulses at $E = +0.2$ V *vs.* the Ag QRE for variable time intervals: (a) 100, (b) 200, and (c) 300 msec. Curve (d) corresponds to the absorbance changes recorded in the absence of an applied potential pulse. All measurements were performed in a HEPES buffer (0.05 M, pH = 7.0) containing (**3**), 1 μM, (**4**), 1 μM, $ABTS^{2-}$, 2 mM, H_2O_2, 2 mM, and hemin 0.5 μM.

formation of the colored product, $ABTS^{\bullet-}$ ($\lambda = 415$ nm). Fig. 3(B) depicts the time-dependent absorbance changes generated by the hemin/G-quadruplex DNAzyme, which is formed upon the electrically-triggered release of Ag^+ ions by voltammetric pulses applied on the electrode for different time intervals. In these experiments, Ag^0 was collected on a Au electrode and acted as a reservoir for Ag^+ ions. The electrode was then subjected to a potential step from −0.6 V to 0.2 V *vs.* the Ag QRE, and the Ag^+ ions were stripped off for different time intervals (100, 200 and 300 ms). The released Ag^+ ions self-assembled the hemin/G-quadruplex DNAzyme structure, and its formation was probed by the catalytic oxidation of $ABTS^{2-}$ by H_2O_2. As the time interval of the applied stripping pulse increased, the DNAzyme-catalyzed oxidation of $ABTS^{2-}$ was enhanced, consistent with the higher content of the DNAzyme generated upon the triggered release of Ag^+, shown in curves (a) to (c). Control experiments revealed that using potential pulses that did not strip off the Ag^+ ions, or in the absence of an applied potential on the electrode, the formation of

the hemin/G-quadruplex was prohibited, as shown by Fig. 3(B), curve (d). The observation of the minor formation of $ABTS^{\bullet-}$ is attributed to the inefficient H_2O_2-stimulated oxidation of $ABTS^{2-}$ by free hemin in the system. In a comparative assay, a series of fixed concentrations of Ag^+ ions were added to the solution containing the two nucleic acids (**3**) and (**4**), and by monitoring the catalytic oxidation of $ABTS^{2-}$ by H_2O_2, the current efficiency corresponding to the electrochemical release of the Ag^+ ions in Fig. 3(B) was estimated to be 76–80%.

The electrical release of Pb^{2+} or Ag^+ ions, and the sequestered activation of DNAzyme-driven transformations reveal the possibility of addressing the electrochemistry of different electrodes and the ability to program catalytic transformations of mixtures of metal ion-controlled DNAzymes. Nonetheless, the fact that the ion release proceeds at different potentials suggests that a single conductive support that contains different metal-ion reservoirs could selectively release one or more ions, depending on the applied potential pulses, thus dictating the subsequent catalytic reactions. Accordingly, the circuit containing the two electrodes functionalized with Pb^0 and Ag^0 was shorted, so that the electrodes could be subjected to the same externally biased potentials. Fig. 4(A) depicts the catalytic properties of the system upon subjecting the two electrodes to an external potential pulse of −0.2 V *vs.* the Ag QRE (time interval 3 s), at which only Pb^{2+} is being released.

The results indicate that under these conditions only the Pb^{2+}-dependent DNAzyme is activated, Fig. 4(A), Panel I, curve (a), while the hemin/G-quadruplex DNAzyme is not formed, as shown by Panel II, curve (a). Fig. 4(B) shows the catalytic functions of the system upon the application of a potential pulse from −0.6 V to 0.2 V. Under these conditions, the two ions Pb^{2+} and Ag^+ ions are released, leading to the activation of the Pb^{2+}-dependent DNAzyme, Fig. 4(B), Panel I, curve (a), and of the hemin/G-quadruplex DNAzyme, Panel II, curve (a).

The systems discussed up to now have demonstrated the electrically-triggered release of metal ions. The reverse uptake of metal ions could, however, switch off the catalytic functions of the DNAzyme, thus introducing an additional means to control the catalytic functions of the cell. The reversible "ON–OFF" electrical switching of the Pb^{2+}-dependent DNAzyme by the cyclic release/uptake of the Pb^{2+} ions is shown in Fig. 5. In these experiments, the Pb^{2+} ions were released from the Pb^0 reservoir associated with the electrode, thus activating the Pb^{2+}-dependent DNAzyme, shown as release point R_1 in Fig. 5, curve (a). At the time marked with U_1, the electrode was biased at −0.95 V *vs.* the Ag QRE (under stirring conditions). The uptake of Pb^{2+} by the electrode resulted in a decrease in the rate of the biocatalytic process, which was significantly but not completely blocked.

The time intervals between ion release (R) and uptake (U) signals were then shortened, resulting in more complete

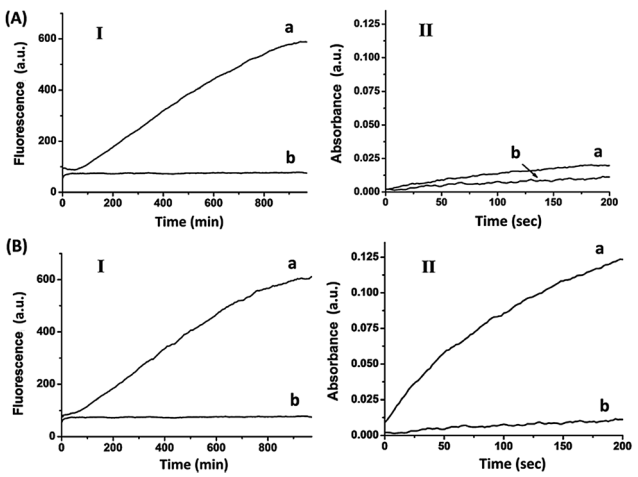

Fig. 4 (A) Time-dependent fluorescence at λ_{em} = 590 nm (Panel I), and time-dependent absorbance at λ = 415 nm (Panel II), corresponding to the electrochemical release of Pb^{2+} ions from the short-circuited Pb- and Ag-deposited Au surfaces: (a) upon the application of a potential pulse at E = −0.2 V *vs.* the Ag QRE for 3 s, (b) in the absence of an applied potential. (B) Time-dependent fluorescence at λ_{em} = 590 nm (Panel I), and time-dependent absorbance at λ = 415 nm (Panel II), corresponding to the electrochemical release of Pb^{2+} and Ag^+ ions from the short-circuited Pb- and Ag-deposited Au surfaces: (a) upon the application of a potential pulse at E = +0.2 V *vs.* the Ag QRE for 3 s, (b) in the absence of an applied potential. All measurements were performed in a HEPES buffer (0.05 M, pH = 7.0) containing (**1**), 1 μM, (**2**), 0.75 μM, (**3**), 1 μM, (**4**), 1 μM, $ABTS^{2-}$, 2 mM, H_2O_2, 2 mM, and hemin 0.5 μM.

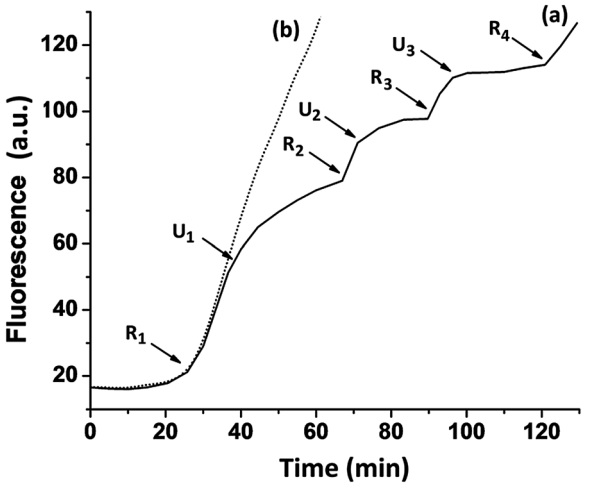

Fig. 5 Time-dependent fluorescence at λ_{em} = 590 nm, corresponding to the electrochemical release (R) of Pb^{2+} ions from the electrode and the activation of the Pb^{2+}-dependent DNAzyme, or the uptake (U) of the Pb^{2+} ions from the DNAzyme-containing solution and their deposition onto the Au surface. Curve (a) corresponds to the intermittent release and uptake of Pb^{2+} ions to and from the solution through the repetitive application of oxidative stripping pulses at −0.2 V *vs.* the Ag QRE for 3 s at the times indicated by the arrows R_{1-4}, and reductive pulses at −0.95 V *vs.* the Ag QRE for 300 s at the times indicated by the arrows U_{1-3}. The measurements were performed under stirring conditions. Curve (b) corresponds to the time-dependent fluorescence changes recorded upon the application of a single oxidation step at −0.2 V *vs.* the Ag QRE for 3 s at the time indicated by the arrow R_1. All measurements were performed in a HEPES buffer (0.05 M, pH = 7.0) containing NaCl, 50 mM, the Pb^{2+}-dependent DNAzyme sequence, (**1**), 1 μM, and the ROX/BH2-functionalized substrate (**2**), 0.75 μM.

blocking. At point R_2, the system was re-subjected to the potential step at −0.2 V, releasing Pb^{2+} ions, which led to the reactivation of the catalytic process. A second reduction pulse was applied at U_2, leading to a further blockage of the biocatalytic process. By the cyclic application of the potential steps to release (R) and uptake (U) the Pb^{2+} ions, the catalytic functions of the system were switched between the "ON"/"OFF" states, respectively. For comparison, Fig. 5, curve (b), shows the continuous catalytic function of the Pb^{2+}-dependent DNAzyme upon the application of a single potential step at −0.2 V for 3 s. Furthermore, the electrically-triggered activation of the Pb^{2+}-dependent DNAzyme was implemented to stimulate a catalytic cascade that synthesizes DNAzyme wires, as shown in Fig. 6(A). In this system, the Pb^0-modified electrode is subjected to a mixture, consisting of the Pb^{2+}-dependent DNAzyme sequence, (**5**), its substrate, (**6**), and two hairpins, H_α (**7**) and H_β (**8**). The fluorophore/quencher-modified substrate of the Mg^{2+}-dependent DNAzyme was also included in the mixture. The hairpins contained the Mg^{2+}-dependent DNAzyme subunits I and II. The

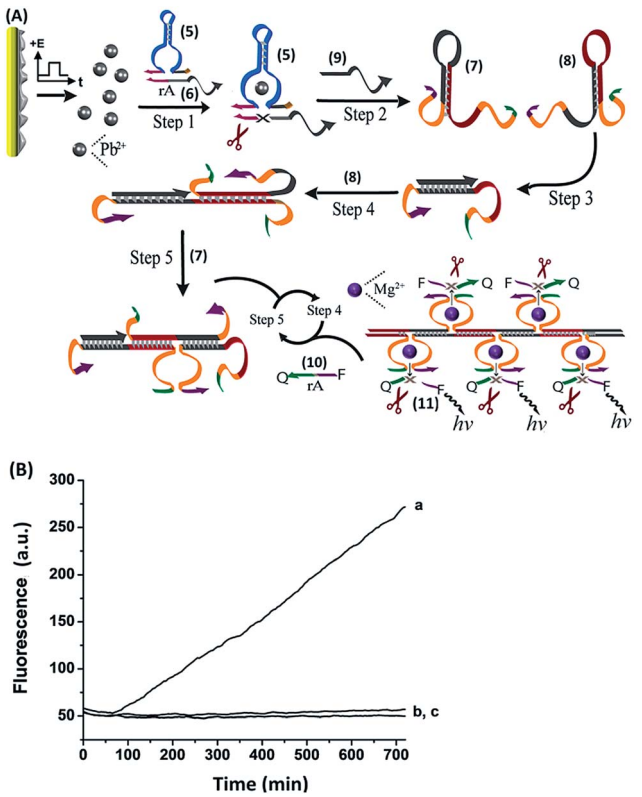

Fig. 6 (A) The electrochemically-triggered activation of a catalytic cascade that synthesizes DNAzyme nanowires through the primary release of Pb^{2+} ions and the subsequent hybridization chain reaction. (B) Time-dependent fluorescence measurements at λ_{em} = 590 nm, corresponding to: (a) the electrochemical release of Pb^{2+} ions from a Pb-deposited Au surface upon the application of a potential pulse at E = −0.2 V *vs.* the Ag QRE for 3 s, (b) time-dependent fluorescence response of the system in the absence of an applied potential pulse to release Pb^{2+} ions, or (c) upon the application of the potential pulse in the absence of the substrate sequence (**6**). All systems included a HEPES buffer (0.1 M, pH = 7.0) containing NaCl, 50 mM, and the DNAs (**5**), 0.2 μM, (**6**), 0.05 μM, (**7**), 3 μM, (**8**), 3 μM, (**10**) 0.75 μM.

electrically-triggered activation of the Pb^{2+}-dependent DNAzyme leads to the cleavage of (**6**) and the fragmented product, (**9**), is complementary to a domain of hairpin H_α. Opening of hairpin H_α drives the hybridization chain reaction (HCR)[36] that results in the cross-opening of hairpins H_α and H_β to yield the polymer wire.

The tethers I and II associated with the polymer wire self-assemble into Mg^{2+}-dependent DNAzyme units[37] that catalyze the cleavage of (**10**). The fluorescence of the fragmented product, (**11**), then provides the readout signal for the DNAzyme cascade. Fig. 6(B), curve (a) depicts the time-dependent fluorescence changes as a result of the operation of the DNAzyme cascade. Control experiments indicate that the Pb^{2+}-dependent DNAzyme sequence, (**5**), and the substrate (**6**), do not activate the DNAzyme cascade in the absence of the electrically-triggered release of Pb^{2+} ions, as shown by curve (b). Similarly, exclusion of the substrate (**6**) from the system does not lead to the activation of the DNAzyme cascade and to the formation of the Mg^{2+}-dependent DNAzymes upon the electrically-triggered release of Pb^{2+} ions, as shown by curve (c). These experiments imply that the primary electrically-triggered release of the Pb^{2+} ions, and the Pb^{2+} ion-dependent DNAzyme cleavage of (**6**), yield the product (**9**) that initiates the HCR process and the formation of the Mg^{2+}-dependent DNAzyme. The electrically-driven activation of the DNAzyme cascade has important implications as it mimics, by electronic triggers, cellular processes, such as addressability, amplification, directed catalytic cascades, and branching of biocatalytic cascades.[1–6]

Methods

Chemicals and Instrumentation

Lead acetate, silver nitrate, hemin and 2,2′-azino-bis(3-ethylbenzothiazoline-6-sulphonic acid) ($ABTS^{2-}$) were purchased from Sigma.

The DNA sequences applied in the study were:

(**1**) 5′-GTCATTTGAAGTAGCGCCGCCGTAACAGTCA-3′

(**2**) 5′-(ROX)-TGACTGTTrAGGAATGAC-(BH2)-3′

(**3**) 5′-TCTCTGTGGAGGG-3′

(**4**) 5′-ACACAGGGACGGG-3′

(**5**) 5′-GTCATTCCTGCTCCTGAAGTAGCGCCGCCGTTCAATTA-3′

(**6**) 5′-AAGACTTCTAATTGArGGAGCAGGAATGAC-3′

(**7**) 5′-GATATCAGCGATCTTCTAATTGAAAGTTATTAATCAATTAGAAGTCTTATGAAGCACCCATGTTACTCT-3′

(**8**) 5′-GATATCAGCGATCTTTTAATAACTTTCAATTAGCATAAGACTTCTAATTGAAAGCACCCATGTTACTCT-3′

(**10**) 5′-(FAM)-AGAGTATrAGGATATC-(BH1)-3′

An Autolab potentiostat (ECO Chemie, the Netherlands) driven by GPES software was used for the electrochemical measurements. A Ag wire (0.5 mm) and a Pt wire (0.5 mm) were used as the quasi-reference (QRE) and counter electrodes, respectively. The cell volume was 200 μL. UV/Visible spectroscopic measurements were performed using a Shimadzu UV-2401 PC spectrophotometer driven by UVProbe 2.33 software. Emission values were recorded using a Carry Eclipsed Fluorescence Spectrophotometer (Agilent Technologies).

Electrode preparation

A clean Au wire (0.5 mm diameter), was immersed in 1 M $HClO_4$ containing lead acetate, 12 mM, and hydroquinone, 70 mM. In order to deposit a dense Pb^0 layer on the Au surface, a potential pulse corresponding to $E = -0.95$ V *vs.* the Ag QRE was applied for 3 minutes under stirring conditions. Similarly, in order to prepare the Ag-modified Au surface, a solution containing silver nitrate, 10 mM in 1 M HNO_3 was used. In this case, a potential pulse corresponding to $E = -0.2$ V *vs.* the Ag QRE was applied for 3 minutes under stirring conditions. The resulting metal-deposited electrodes were carefully washed using HNO_3 and copious amounts of water. The release of the metal ions from the modified surfaces was performed using an *in situ* procedure, in which the target DNA sequences were presented in the electrochemical cells during the application of the oxidative potential pulses. The cells were assembled inside standard plastic cuvettes, which were subsequently used for measuring the fluorescence and absorbance spectra associated with the different DNA systems.

Conclusions

To conclude, the present study has introduced the first steps for the development of an artificial "electronic cell". It was demonstrated that the electrochemical release of ions was coupled to the subsequent activation of the catalytic functions of DNAzymes and DNAzyme cascades. The formation of the DNAzymes translated the electronic stimuli into chemical transformations and provided amplification of the electrochemical triggers. Also, the ON/OFF switching of the electronically-triggered DNAzyme functions demonstrated a means to electrically control the extent of the biocatalytic transformations. Such control could be linked to the electrochemical sensors of specific DNA or other cell concentrations to provide regulated "metabolic" feedback between the progress of artificial cell reactions and the initiation of further phases of the cell cycle.

Acknowledgements

This research is supported by the EU FET Open MICREAgents Project # 318671.

Notes and references

1 A. Pohorille and D. Deamer, *Trends Biotechnol.*, 2002, **20**, 123–128.
2 G. Murtas, *Mol. BioSyst.*, 2009, **5**, 1292–1297.
3 A. C. Forster and G. M. Church, *Mol. Syst. Biol.*, 2006, **2**, 45.
4 G. Murtas, *Origins Life Evol. Biospheres*, 2007, **37**, 419–422.
5 A. V. Pietrini and P. L. Luisi, *ChemBioChem*, 2004, **5**, 1055–1062.
6 J. W. Szostak, D. P. Bartel and P. L. Luisi, *Nature*, 2001, **409**, 387–390.
7 P. L. Luisi, F. Ferri and P. Stano, *Naturwissenschaften*, 2006, **93**, 1–13.
8 K. Ishikawa, K. Sato, Y. Shima, I. Urabe and T. Yomo, *FEBS Lett.*, 2004, **576**, 387–390.
9 G. Murtas, Y. Kuruma, P. Bianchini, A. Diaspro and P. L. Luisi, *Biochem. Biophys. Res. Commun.*, 2007, **363**, 12–17.
10 V. Noireaux and A. Libchaber, *Proc. Natl. Acad. Sci U. S. A.*, 2004, **101**, 17669–17674.
11 I. Vilotijevic and T. F. Jamison, *Angew. Chem., Int. Ed.*, 2009, **48**, 5250–5281.
12 P. Walde, R. Wick, M. Fresta, A. Mangone and P. L. Luisi, *J. Am. Chem. Soc.*, 1994, **116**, 11649–11654.
13 P. K. Schmidli, P. Schurtenberger and P. L. Luisi, *J. Am. Chem. Soc.*, 1991, **113**, 8127–8130.
14 P. F. Wagler, U. Tangen, T. Maeke and J. S. McCaskill, *BioSystems*, 2012, **109**, 2–17.
15 Y. Xiao, V. Pavlov, T. Niazov, A. Dishon, M. Kolter and I. Willner, *J. Am. Chem. Soc.*, 2004, **126**, 7430–7431.
16 D. M. Kolpashchikov, *J. Am. Chem. Soc.*, 2008, **130**, 2934–2935.
17 F. Wang, J. Elbaz, C. Teller and I. Willner, *Angew. Chem., Int. Ed.*, 2011, **50**, 295–299.
18 G. Pelossof, R. Tel-Vered and I. Willner, *Anal. Chem.*, 2012, **84**, 3703–3709.
19 T. Li, L. Shi, E. Wang and S. Dong, *Chem.–Eur. J.*, 2009, **15**, 1036–1042.
20 Y. Weizmann, M. K. Beissenhirtz, Z. Cheglakov, R. Nowaski, M. Kolter and I. Willner, *Angew. Chem., Int. Ed.*, 2006, **45**, 7384–7388.
21 Y. Tian, Y. He and C. Mao, *ChemBioChem*, 2006, **7**, 1862–1864.
22 Z. Cheglakov, Y. Weizmann, B. Basnar and I. Willner, *Org. Biomol. Chem.*, 2007, **5**, 223–225.
23 F. Wang, J. Elbaz, R. Orbach, N. Magen and I. Willner, *J. Am. Chem. Soc.*, 2011, **133**, 17149–17151.
24 B. Cuenoud and J. W. Szostak, *Nature*, 1995, **375**, 611–614.
25 K. B. Chapman and J. W. Szostak, *Chem. Biol.*, 1995, **2**, 325–333.
26 R. R. Breaker and G. F. Joyce, *Chem. Biol.*, 1994, **1**, 223–229.
27 P. Travascio, Y. Li and D. Sen, *Chem. Biol.*, 1998, **5**, 505–517.
28 S. Nakayama and H. O. Sintim, *J. Am. Chem. Soc.*, 2009, **131**, 10320–10333.
29 E. Golub, R. Freeman and I. Willner, *Angew. Chem., Int. Ed.*, 2011, **50**, 11710–11714.
30 A. K. Brown, J. Li, C. M. B. Pavot and Y. Lu, *Biochemistry*, 2003, **42**, 7152–7161.
31 J. Liu and Y. Lu, *Anal. Chem.*, 2003, **75**, 6666–6672.
32 H. K. Kim, J. Liu, J. Li, N. Nagraj, M. Li, C. M. B. Pavot and Y. Lu, *J. Am. Chem. Soc.*, 2007, **129**, 6896–6902.
33 C. K. Chiang, C. C. Huang, C. W. Liu and H. T. Chang, *Anal. Chem.*, 2008, **80**, 3716–3721.
34 D. M. Kolpashchikov, *J. Am. Chem. Soc.*, 2008, **130**, 2934–2935.
35 J. Elbaz, M. Moshe, B. Shlyahovsky and I. Willner, *Chem.–Eur. J.*, 2009, **15**, 3411–3418.
36 R. M. Dirks and N. A. Pierce, *Proc. Natl. Acad. Sci. U. S. A.*, 2004, **101**, 15275–15278.
37 R. R. Breaker and G. F. Joyce, *Chem. Biol.*, 1995, **2**, 655–660.